Robust Joint Design of Waveform and Mismatched Filter for ISRJ Suppression via Stochastic Majorization Minimization

Youwei Yuan, Yongzhe Li, and Ran Tao
School of Information and Electronics, Beijing Institute of Technology, Beijing 100081, China
Emails: youwei.yuan@bit.edu.cn, lyz@ieee.org/yongzhe.li@bit.edu.cn, rantao@bit.edu.cn

***Abstract*—In this paper, we propose a joint design of a unimodular waveform and a mismatched filter to suppress interrupted sampling repeater jamming (ISRJ).The goal of our design is to achieve high target detection accuracy, effective ISRJ suppression, and robustness against variations in ISRJ forwarding times, while effectively controlling signal-to-noise ratio loss caused by mismatched filter. To satisfy all the aforementioned requirements, we employ a weighted sum of three metrics related to integrated sidelobe level, jamming integrated level, and signal-to-interference-plus-noise ratio as the objective. Based on this, we formulate the joint design as a non-convex optimization problem with constraints on waveform modulus, filtering energy and mainlobe peak level. To address this problem, we reformulate the optimization as minimizing the expected value of the objective over ISRJ forwarding times and apply the stochastic majorization-minimization technique. This approach involves sampling ISRJ forwarding times from the specified interval and systematically transforming the reformulated problem into a sequence of distinct sub-problems based on these samples. Our contributions also lie in elaborating the majorant for each sub-problem and deriving a closed-form solution. Simulation results verify the effectiveness of the proposed design.**

***Index Terms*—Interrupted sampling repeater jamming (ISRJ), robust joint design, stochastic majorization minimization (SMM).**

I. Introduction

Interrupted sampling repeater jamming (ISRJ) has emerged as a major issue in radar applications. This jamming technique generates a series of false targets after pulse compression, effectively masking real targets [1]. Consequently, ISRJ suppression has become a prominent research topic in recent years [1]–[3]. Traditionally, the primary focus of ISRJ suppression is to counter both the barrage and deception effects. However, the increasing complexity of jamming patterns and the variability of jamming parameters have made accurate target detection significantly more challenging. To handle these issues, extensive studies have been devoted to ISRJ suppression, with advanced approaches continuing to be developed.

To address the significant challenges posed by ISRJ, numerous studies on ISRJ suppression have been reported [4]–[11]. Early works mainly focus on passive jamming mitigation at the receive end [4], utilizing feature-based analysis tools to identify and suppress jamming components. However, these methods do not guarantee the quality of transmitted waveforms, such as good correlation levels and high resolution. To address this problem, strategies based on waveform design [5], [6] or joint design of waveforms and receive filters [7]–[10] have been employed. The joint design approach, which leverages waveform agility and mismatched filtering, provides additional degrees of freedom for the design task and achieves better jamming suppression capability compared to designing waveform or filter alone. Technically, many works focus on minimizing integrated sidelobe level (ISL) [7]–[9] or peak sidelobe level to enhance jamming suppression capability [10]. However, the aforementioned methods heavily rely on accurate estimation of jamming parameters, limiting their effectiveness in highly dynamic or uncertain environments. To tackle this issue, some recent works have explored the extended waveform domain [11]. However, the joint design method with robustness against uncertain jamming parameters and excellent correlation properties has rarely been studied in existing literature.

In this paper, we propose a joint design of the unimodular waveform and the mismatched filter for ISRJ suppression, which can adapt to ISRJ forwarding times that are distributed within a specific interval and follow an unknown distribution. We aim to achieve excellent target detection and jamming suppression capabilities, while maintaining robustness against ISRJ forwarding times. To this end, we formulate a joint design that minimizes a weighted sum of three metrics related to ISL, JIL, and SINR as a non-convex problem with constraints on SNRL and mainlobe peak level. Then, we reformulate the objective as an expectation form and iteratively decompose the non-convex problem into a set of tractable sub-problems using samples of ISRJ forwarding times. To solve it, we choose a proper majorant for each sub-problem and finally derive a closed-form solution via SMM technique [12]. Simulation results verify the superiority of our method.

Notations: We use $|\cdot|$, $\|\cdot\|$, $(\cdot)^*$, $(\cdot)^{\mathrm{T}}$, $(\cdot)^{\mathrm{H}}$, $\mathrm{tr}\{\cdot\}$, $\mathrm{vec}(\cdot)$, $\Re\{\cdot\}$, $\arg(\cdot)$, $\lambda_{\max}(\cdot)$, $\mathbb{E}_m\{\cdot\}$, $\odot$, and $\otimes$ to denote modulus, Euclidean norm, conjugate, transpose, conjugate transpose, matrix trace, column-wise vectorization, real part, argument of a complex vector, largest eigenvalue of a matrix, mathematical expectation with respect to a random variable m, Hadamard product, and Kronecker product, respectively. In addition, $\mathbf{I}_N$ and $\mathbf{1}_N$ denote the $N \times N$ identity matrix and the N-length vector of all ones, respectively.

This work was supported in part by the National Natural Science Foundation of China (NSFC) under grants 62271054 and U21A20456.

II. Signal Model and Problem Formulation

Let us consider the design of a unimodular waveform of code length N. We denote the waveform vector by $\mathbf{x} \triangleq [x(1), \ldots, x(N)]^{\mathrm{T}} \in \mathbb{C}^{N\times 1}$, whose n-th element is expressed as $e^{j\psi(n)}$. Here, $\psi(n)$ is the phase of the n-th element, which takes an arbitrary value ranging between $-\pi$ and π.

The ISRJ signal serves as a discretized and repeated version of the transmitted waveform, generated by sampling and repeatedly forwarding intercepted slices. To mathematically express the sampling and forwarding methods of ISRJ generation, we use $\mathbf{\Phi}_m \triangleq \mathbf{I}_P \otimes \mathbf{A}_m$ with $\mathbf{A}_m \triangleq [0, \mathbf{0}_{1\times m}; \mathbf{1}_{m\times 1}, \mathbf{0}_{m\times m}] \in \mathbb{R}^{(1+m)\times(1+m)}$ to denote the ISRJ pattern matrix with respect to forwarding times m. Here, P is the number of sampling slices, satisfying $P(1+m) = N$. Based on this, the ISRJ signal can be expressed as the product of the pattern matrix and transmitted waveform, which is given by

$$\tilde{\mathbf{x}}_m = \mathbf{\Phi}_m \mathbf{x} \tag{1}$$

with $m \in \mathcal{M}$ and $\mathcal{M} \triangleq \{1, \ldots, N-1\}$ being the set of possible values of ISRJ forwarding times.

At the receive end, considering the target and jamming components, and stacking the data into a vector, the overall receive data vector $\mathbf{r} \in \mathbb{C}^{N\times 1}$ can be expressed as

$$\mathbf{r} = \alpha_t \mathbf{x} + \alpha_j \tilde{\mathbf{x}}_m + \mathbf{n} \tag{2}$$

where α_t and α_j denote the complex amplitudes of echoes from the target and jammer, respectively. Here, $\mathbf{n} \in \mathbb{C}^{N\times 1}$ is the noise vector satisfying $\mathbf{n} \sim \mathcal{CN}(0, \sigma_n^2)$, with σ_n^2 being its variance. Subsequently, the mismatched filter with the weight vector $\mathbf{w} \in \mathbb{C}^{N\times 1}$ is applied to the received data vector $\mathbf{r}$. Hence, the signal-to-interference-plus-noise ratio (SINR) at the output of the filter can be expressed as

$$\zeta_{\mathrm{SINR}} \triangleq \frac{|\alpha_t|^2 \cdot |\mathbf{w}^{\mathrm{H}}\mathbf{x}|^2}{|\alpha_j|^2 |\mathbf{w}^{\mathrm{H}}\tilde{\mathbf{x}}_m|^2 + \sigma_n^2 \mathbf{w}^{\mathrm{H}}\mathbf{w}}. \tag{3}$$

The design is expected to exhibit good correlation properties, thereby ensuring accurate extraction of real targets of interest. To this end, we use the integrated sidelobe level (ISL) metric to evaluate sidelobe suppression capability, defined as

$$\zeta_{\mathrm{ISL}} \triangleq \sum_{l\in\Omega_s} |\mathbf{w}^{\mathrm{H}}\mathbf{J}_l\mathbf{x}|^2 \tag{4}$$

where Ω_s represents the discrete delay set of the sidelobe region and $\mathbf{J}_l \triangleq \left[\mathbf{0}_{l\times(N-l)}, \mathbf{I}_{l\times l}; \mathbf{0}_{(N-l)\times(N-l)}, \mathbf{0}_{(N-l)\times l}\right] \in \mathbb{R}^{N\times N}$.

Meanwhile, the design is also expected to have excellent anti-ISRJ capability. To this end, we employ the jamming integrated level (JIL) metric to characterize the ISRJ suppression performance, which is given by

$$\zeta_{\mathrm{JIL}} \triangleq \sum_{l\in\Omega} |\mathbf{w}^{\mathrm{H}}\mathbf{J}_l\tilde{\mathbf{x}}_m|^2 \tag{5}$$

where Ω represents the set of all discrete delays.

We aim to simultaneously suppress ISRJ and ensure radar detection performance with robustness to variable ISRJ forwarding times. To this end, the aforementioned metrics in (3), (4), and (5) are of interest. Consequently, we employ the weighted sum of ζ_{ISL}, ζ_{JIL}, and $1/\zeta_{\mathrm{SINR}}$ as the objective function, whose expression is given by

$$\begin{aligned}\zeta(\mathbf{x}, \mathbf{w}, m) &\triangleq \tilde{\delta}(\epsilon\, \zeta_{\mathrm{ISL}} + (1-\epsilon)\, \zeta_{\mathrm{JIL}}) + (1-\delta)(1/\zeta_{\mathrm{SINR}}) \\ &= \tilde{\delta}\big(\epsilon \sum_{l\in\Omega_s} |\mathbf{w}^{\mathrm{H}}\mathbf{J}_l\mathbf{x}|^2 + (1-\epsilon)\sum_{l\in\Omega} |\mathbf{w}^{\mathrm{H}}\mathbf{J}_l\mathbf{\Phi}_m\mathbf{x}|^2\big) \\ &\quad + (1-\delta)\,\frac{|\alpha_j|^2\,|\mathbf{w}^{\mathrm{H}}\mathbf{\Phi}_m\mathbf{x}|^2 + \sigma_n^2\mathbf{w}^{\mathrm{H}}\mathbf{w}}{|\alpha_t|^2|\mathbf{w}^{\mathrm{H}}\mathbf{x}|^2}\end{aligned} \tag{6}$$

where δ and ϵ denote the weighting factors, $\tilde{\delta} \triangleq \delta/N^2$. Here, the second equality is derived by substituting (1), (3), (4), and (5) into the first equality of (6).

The signal-to-noise ratio loss (SNRL) caused by the mismatched filter is also crucial for radar systems to detect weak targets, and it is expected to maintain a specified level. To this end, we use ζ_{SNRL} to evaluate the gain loss, defined as

$$\zeta_{\mathrm{SNRL}} \triangleq 10\log_{10}\left(\frac{|\mathbf{w}^{\mathrm{H}}\mathbf{x}|^2}{(\mathbf{w}^{\mathrm{H}}\mathbf{w})\,(\mathbf{x}^{\mathrm{H}}\mathbf{x})}\right). \tag{7}$$

The goal of the design is to find a solution that minimizes $\zeta(\mathbf{x}, \mathbf{w}, m)$ while guaranteeing good SNRL performance. To this end, we propose the joint design given as follows[1]

$$\begin{aligned}\min_{\mathbf{x},\mathbf{w},\forall m\in\mathcal{M}} \quad & \zeta(\mathbf{x}, \mathbf{w}, m) && \text{(8a)}\\ \text{s.t.} \quad & \mathbf{w}^{\mathrm{H}}\mathbf{x} = N && \text{(8b)}\\ & \|\mathbf{w}\|^2 = \gamma_0 N && \text{(8c)}\\ & |\mathbf{x}| = 1 && \text{(8d)}\end{aligned}$$

where the constraint (8b) controls the mainlobe peak level, the constraint (8c) restricts the power of mismatched filter to a constant $\gamma_0 N$, and the constraint (8d) guarantees the constant-modulus property for each waveform element. Based on (8b)-(8d), the SNRL metric in (7) can be precisely controlled by adjusting γ_0, i.e., $\zeta_{\mathrm{SNRL}} = -10\log_{10}(\gamma_0)$.

III. Efficient joint Design VIA Stochastic Majorization Minimization

Considering that the ISRJ forwarding times m in (8) are randomly distributed in a specific range following an unknown distribution, we exploit the idea of SMM [12] to handle the non-convexity and parametric uncertainty of (8). Specifically, we first reformulate the objective (8a) as an expectation with respect to ISRJ forwarding times, whose optimization variable is redefined as a joint sequence of the waveform and filter. Then, we obtain a set of samples from the known interval of ISRJ forwarding times, and iteratively select individual sample points from this set to construct sub-problems, each corresponding to a specific sample point. Based on this, we iteratively decompose the expectation-based problem into a series of distinct sub-problems. For each sub-problem, we transform its quartic objective into a quadratic form, based on which we derive a proper majorant for the reformulated objective. Then, we update the approximate majorant, which is

[1]Here, the modulus $|\cdot|$ is applied to a vector argument, whose calculation is conducted on each individual element of the input vector. The same type of operations for $e^{j(\cdot)}$ and $\arg(\cdot)$ are used throughout the paper.

in fact a weighted average of previously computed majorants. By minimizing the approximate majorant and projecting the constraints onto corresponding feasibility sets, we can finally derive a closed-form solution. In the following, we elaborate the specific procedures for solving (8).

Since the ISRJ forwarding times m typically vary with the jammers in practice, we consider optimizing the expected form of (8a) to enhance the robustness of the joint design against varying ISRJ forwarding times. To this end, we use $\tilde{\zeta}(\mathbf{x},\mathbf{w}) \triangleq \mathbb{E}_m\{\zeta(\mathbf{x},\mathbf{w},m)\}$ with $m \in \mathcal{M}$ to denote the expectation-based objective. For simplicity, we optimize both the transmitted waveform and the mismatched filter simultaneously, i.e., $\mathbf{y} \triangleq \left[\mathbf{w}^{\mathrm{T}},\mathbf{x}^{\mathrm{T}}\right]^{\mathrm{T}} \in \mathbb{C}^{2N\times 1}$. Hence, we can rewrite the expectation-based objective $\tilde{\zeta}(\mathbf{x},\mathbf{w})$ as follows

$$\begin{aligned}\tilde{\zeta}(\mathbf{y}) = \tilde{\delta}\big(\epsilon \sum_{l\in\Omega_s} |\mathbf{y}^{\mathrm{H}}\tilde{\mathbf{J}}_l\mathbf{y}|^2 + (1-\epsilon)\mathbb{E}_m\big\{\sum_{l\in\Omega} |\mathbf{y}^{\mathrm{H}}\mathbf{V}_{l,m}\mathbf{y}|^2\big\}\big) \\ + (1-\delta)\,\mathbb{E}_m\big\{|\mathbf{y}^{\mathrm{H}}\mathbf{V}_{0,m}\mathbf{y}|^2\big\} \end{aligned} \tag{9}$$

where $\tilde{\mathbf{J}}_l \triangleq [\mathbf{0}_{N\times N},\mathbf{J}_l;\mathbf{0}_{N\times N},\mathbf{0}_{N\times N}] \in \mathbb{R}^{2N\times 2N}$, $\mathbf{V}_{l,m} \triangleq \tilde{\mathbf{\Phi}}_m^{\mathrm{H}}\tilde{\mathbf{J}}_l\tilde{\mathbf{\Phi}}_m$ with $\tilde{\mathbf{\Phi}}_m \triangleq [\mathbf{I}_{N\times N},\mathbf{0}_{N\times N};\mathbf{0}_{N\times N},\mathbf{\Phi}_m] \in \mathbb{R}^{2N\times 2N}$. Based on this, the expectation-based problem is written as

$$\begin{aligned} \min_{\mathbf{y}} \quad & \tilde{\zeta}(\mathbf{y}) && (10a)\\ \text{s.t.} \quad & \mathbf{y}^{\mathrm{H}}\tilde{\mathbf{J}}_0\mathbf{y} = N && (10b)\\ & \|\mathbf{y}\odot\mathbf{u}\|^2 = \gamma_0 N && (10c)\\ & |\mathbf{y}\odot\tilde{\mathbf{u}}| = 1 && (10d)\end{aligned}$$

where $\mathbf{u} \triangleq \left[\mathbf{1}_N^{\mathrm{T}},\mathbf{0}_N^{\mathrm{T}}\right]^{\mathrm{T}} \in \mathbb{R}^{2N\times 1}$ and $\tilde{\mathbf{u}} \triangleq \left[\mathbf{0}_N^{\mathrm{T}},\mathbf{1}_N^{\mathrm{T}}\right]^{\mathrm{T}} \in \mathbb{R}^{2N\times 1}$.

We adopt an iterative approach to solving (10) using a cyclic algorithm based on the SMM framework, which optimizes the objective over one specific sample at each iteration. Specifically, we first choose K samples of ISRJ forwarding times m from $\mathcal{M}$, denoted as $\{m_k \in \mathcal{M}\}_{k=1}^K$. Then, we select the k-th sample point m_k from the set at the k-th iteration to formulate the k-th sub-problem. Moreover, we use the penalty function method to address the constraint (10b). Therefore, the k-th sub-problem of (10) with $m = m_k$ can be expressed as

$$\begin{aligned} \min_{\mathbf{y}} \quad & \tilde{\zeta}(\mathbf{y})|_{m=m_k} + \lambda_0|\mathbf{y}^{\mathrm{H}}\tilde{\mathbf{J}}_0\mathbf{y} - N|^2 && (11a)\\ \text{s.t.} \quad & \|\mathbf{y}\odot\mathbf{u}\|^2 = \gamma_0 N && (11b)\\ & |\mathbf{y}\odot\tilde{\mathbf{u}}| = 1 && (11c)\end{aligned}$$

where λ_0 is the penalty factor.

In order to solve (11), we adopt the idea of selecting a proper majorant for its objective, and then solve the corresponding problem by means of SMM technique. Since the procedure is the same for each value of m, the index m is omitted for brevity. Before handling (11), we present the following lemma.

Lemma 1. *If a real-valued function $f(\mathbf{z})$ with respect to a complex variable $\mathbf{z} \in \mathbb{C}^{N\times 1}$ takes a quartic form, i.e., $f(\mathbf{z}) = |\mathbf{z}^{\mathrm{H}}\mathbf{L}\mathbf{z}|^2$ with $|\mathbf{z}| = 1$, the following function*

$$\begin{aligned} g(\mathbf{z}) = 2\Re\Big\{\mathbf{z}^{\mathrm{H}}\Big((\mathbf{z}_0^{\mathrm{H}}\mathbf{L}\mathbf{z}_0)^*\,\mathbf{L} + \mathbf{z}_0^{\mathrm{H}}\mathbf{L}\mathbf{z}_0\,\mathbf{L}^{\mathrm{H}} - 2\lambda_{\max}\big(\mathrm{vec}(\mathbf{L}) \\ \times \mathrm{vec}^{\mathrm{H}}(\mathbf{L})\big)\,\mathbf{z}_0\mathbf{z}_0^{\mathrm{H}} - 2\,\big|\mathbf{z}_0^{\mathrm{H}}\mathbf{L}\mathbf{z}_0\big|\,\mathbf{I}_N\Big)\mathbf{z}_0\Big\} \end{aligned} \tag{12}$$

Algorithm 1 Joint Design Algorithm via SMM

1: Initialization: $\mathbf{y}^{(0)}$, K, β_k, $\tilde{\mathbf{s}}^{(0)} \leftarrow \mathbf{y}^{(0)}$, $\bar{\mathbf{s}}^{(0)} \leftarrow \mathbf{y}^{(0)}$.
2: **for** $k = 1 : K$ **do**
3: Draw a sample $m_k \in \mathcal{M}$ and calculate $\mathbf{Q}^{(k)}$ via (16).
4: Update $\mathbf{s}^{(k)}$, $\tilde{\mathbf{s}}^{(k)}$, $\bar{\mathbf{s}}^{(k)}$, and $\mathbf{y}^{(k)}$ via (21)-(25).
5: **end for**

serves as a majorant for $f(\mathbf{z})$ at any given $\mathbf{z}_0 \in \mathbf{dom}(f)$.

Proof. For brevity, let us denote $\mathbf{Z} \triangleq \mathbf{z}\mathbf{z}^{\mathrm{H}}$ and $\tilde{\mathbf{L}} \triangleq \mathrm{vec}(\mathbf{L})\mathrm{vec}^{\mathrm{H}}(\mathbf{L})$ to facilitate derivation. Since $\mathbf{z}^{\mathrm{H}}\mathbf{L}\mathbf{z} = \mathrm{tr}\{\mathbf{L}\mathbf{Z}\}$ and $\mathrm{tr}\{\mathbf{L}\mathbf{Z}\} = \mathrm{vec}^{\mathrm{H}}(\mathbf{Z})\mathrm{vec}(\mathbf{L})$, we can rewrite $f(\mathbf{z})$ into a quadratic form, given by $f(\mathbf{z}) = \mathrm{vec}^{\mathrm{H}}(\mathbf{Z})\tilde{\mathbf{L}}\mathrm{vec}(\mathbf{Z})$. Using the fact that a quadratic form $\mathbf{c}^{\mathrm{H}}\mathbf{D}\mathbf{c}$ can be majorized at any given point $\mathbf{c}_0$ in its feasibility set by $\mathbf{c}^{\mathrm{H}}\mathbf{G}\mathbf{c} + 2\Re\{\mathbf{c}^{\mathrm{H}}(\mathbf{D}-\mathbf{G})\mathbf{c}_0\} + \mathbf{c}_0^{\mathrm{H}}(\mathbf{G}-\mathbf{D})\mathbf{c}_0$ [13] and enforcing $\mathbf{c} \triangleq \mathrm{vec}(\mathbf{Z})$, $\mathbf{c}_0 \triangleq \mathrm{vec}(\mathbf{Z}_0)$, $\mathbf{D} \triangleq \tilde{\mathbf{L}}$, and $\mathbf{G} \triangleq \lambda_{\max}(\tilde{\mathbf{L}})\,\mathbf{I}_N$, we can derive that

$$\begin{aligned} f(\mathbf{z}) = \mathrm{vec}^{\mathrm{H}}(\mathbf{Z})\tilde{\mathbf{L}}\mathrm{vec}(\mathbf{Z}) \le \mathrm{vec}^{\mathrm{H}}(\mathbf{Z})\mathbf{G}\mathrm{vec}(\mathbf{Z}) + \mathrm{vec}^{\mathrm{H}}(\mathbf{Z}_0) \\ \times (\mathbf{G}-\tilde{\mathbf{L}})\mathrm{vec}(\mathbf{Z}_0) + 2\Re\big\{\mathrm{vec}^{\mathrm{H}}(\mathbf{Z})(\tilde{\mathbf{L}}-\mathbf{G})\mathrm{vec}(\mathbf{Z}_0)\big\} \end{aligned} \tag{13}$$

with $\mathbf{Z}_0 \triangleq \mathbf{z}_0\mathbf{z}_0^{\mathrm{H}}$. Substituting $\mathrm{vec}^{\mathrm{H}}(\mathbf{Z})\tilde{\mathbf{L}}\mathrm{vec}(\mathbf{Z}_0) = \mathrm{tr}\{\mathbf{Z}^{\mathrm{H}}\mathbf{L}\}\,\mathrm{tr}\{\mathbf{L}^{\mathrm{H}}\mathbf{Z}_0\}$ and $2\Re\{(\mathbf{z}_0^{\mathrm{H}}\mathbf{L}\mathbf{z}_0)^*\,\mathbf{z}^{\mathrm{H}}\mathbf{L}\mathbf{z}\} = \mathbf{z}^{\mathrm{H}}\hat{\mathbf{L}}\mathbf{z}$ with $\hat{\mathbf{L}} \triangleq (\mathbf{z}_0^{\mathrm{H}}\mathbf{L}\mathbf{z}_0)^*\,\mathbf{L} + \mathbf{z}_0^{\mathrm{H}}\mathbf{L}\mathbf{z}_0\,\mathbf{L}^{\mathrm{H}}$ into (13), the majorant for $f(\mathbf{z})$ at any point $\mathbf{z}_0 \in \mathbf{dom}(f)$ can be rewritten as $f(\mathbf{z}) \le \mathbf{z}^{\mathrm{H}}\big(\hat{\mathbf{L}} - 2\lambda_{\max}(\tilde{\mathbf{L}})\mathbf{z}_0\mathbf{z}_0^{\mathrm{H}}\big)\,\mathbf{z}$, which can be further majorized by

$$g(\mathbf{z}) = 2\Re\big\{\mathbf{z}^{\mathrm{H}}\big(\hat{\mathbf{L}} - 2\lambda_{\max}(\tilde{\mathbf{L}})\mathbf{z}_0\mathbf{z}_0^{\mathrm{H}} - 2\,\big|\mathbf{z}_0^{\mathrm{H}}\mathbf{L}\mathbf{z}_0\big|\,\mathbf{I}_N\big)\mathbf{z}_0\big\} \tag{14}$$

by enforcing $\mathbf{c} \triangleq \mathbf{z}$, $\mathbf{c}_0 \triangleq \mathbf{z}_0$, $\mathbf{D} \triangleq \hat{\mathbf{L}} - 2\lambda_{\max}(\tilde{\mathbf{L}})\mathbf{z}_0\mathbf{z}_0^{\mathrm{H}}$, and $\mathbf{G} \triangleq 2\,\big|\mathbf{z}_0^{\mathrm{H}}\mathbf{L}\mathbf{z}_0\big|\,\mathbf{I}_N$. The majorant in (14) has the same form as (12) after substituting the explicit expression of the matrices $\hat{\mathbf{L}}$ and $\tilde{\mathbf{L}}$ back. The proof is complete. □

We apply Lemma 1 to (11a) for the elaboration of its majorant. Toward this end, we present the following result.

Lemma 2. *The majorant for* (11a) *takes the form given by*

$$g(\mathbf{y}) = 2\Re\{\mathbf{y}^{\mathrm{H}}\mathbf{Q}^{(k)}\,\mathbf{y}^{(k-1)}\} \tag{15}$$

where $\mathbf{y}^{(k-1)}$ denotes the sequence obtained by solving the sub-problem at the last iteration, and

$$\begin{aligned} \mathbf{Q}^{(k)} \triangleq \epsilon\tilde{\delta}\,\mathcal{T}\{\mathbf{y}^{(k-1)},\tilde{\mathbf{J}}_l,\Omega_s\} + (1-\varepsilon)\tilde{\delta}\,\mathcal{T}\{\mathbf{y}^{(k-1)},\mathbf{V}_l,\Omega\} \\ +(1-\delta)\mathcal{T}\{\mathbf{y}^{(k-1)},\mathbf{V}_0,\{0\}\} + \lambda_0\mathcal{T}\{\mathbf{y}^{(k-1)},\tilde{\mathbf{J}}_0,\{0\}\} \end{aligned} \tag{16}$$

with $\mathcal{T}\{\cdot,\cdot,\cdot\}$ being the operator that denotes the repeated calculation involved in the majorant for (11a)*. Taking $\mathcal{T}\{\cdot,\cdot,\cdot\}$ with the first set of input parameters on the right-hand side of* (16) *as an example, we enforce its definition given by*

$$\begin{aligned} \mathcal{T}\big\{\mathbf{y}^{(k-1)},\tilde{\mathbf{J}}_l,\Omega_s\big\} \triangleq \sum_{l\in\Omega_s}\Big(\big((\mathbf{y}^{(k-1)})^{\mathrm{H}}\tilde{\mathbf{J}}_l\mathbf{y}^{(k-1)}\big)^*\tilde{\mathbf{J}}_l \\ + (\mathbf{y}^{(k-1)})^{\mathrm{H}}\tilde{\mathbf{J}}_l\mathbf{y}^{(k-1)}\tilde{\mathbf{J}}_l^{\mathrm{H}}\Big) - 2N\mathbf{y}^{(k-1)}(\mathbf{y}^{(k-1)})^{\mathrm{H}} \\ - \sum_{l\in\Omega_s} 2\big|(\mathbf{y}^{(k-1)})^{\mathrm{H}}\tilde{\mathbf{J}}_l\mathbf{y}^{(k-1)}\big|. \end{aligned} \tag{17}$$

The other operators in (16) *can be obtained from the example*

TABLE I

PERFORMANCE COMPARISONS VERSUS DIFFERENT CODE LENGTHS.

	$N=32$				$N=64$				$N=128$			
	ISL[a]	JIL	JPL	SINR	ISL	JIL	JPL	SINR	ISL	JIL	JPL	SINR
MIAJS-MM	−0.79 dB	−5.92 dB	−17.98 dB	19.42 dB	−0.64 dB	−7.64 dB	−20.63 dB	20.34 dB	−1.32 dB	−9.42 dB	−25.16 dB	22.16 dB
DCADPM	−1.42 dB	−8.74 dB	−20.18 dB	17.83 dB	−1.85 dB	−9.46 dB	−21.85 dB	19.92 dB	−2.26 dB	−10.38 dB	−27.63 dB	23.49 dB
Proposed	−2.89 dB	−11.82 dB	−23.40 dB	23.63 dB	−2.52 dB	−12.65 dB	−25.38 dB	25.13 dB	−3.46 dB	−14.96 dB	−31.54 dB	29.93 dB

[a] Normalized PSL value obtained after iterations (in dBs). The same operations for ISL, JIL, JPL, and SINR values are applied in all tables.

TABLE II

JIL PERFORMANCE OF THE ALGORITHMS TESTED VERSUS DIFFERENT ISRJ FORWARDING TIMES.

	$m=10$	$m=15$	$m=20$	$m=25$	$m=30$	$m=35$	$m=40$	$m=45$	$m=50$	$m=55$	$m=60$
JDA-ADMM	−6.67 dB	−7.26 dB	−9.67 dB	−11.56 dB	−12.72 dB	−18.47 dB	−12.53 dB	−12.16 dB	−10.32 dB	−9.58 dB	−9.37 dB
MIAJS-MM	−10.74 dB	−10.98 dB	−11.43 dB	−11.26 dB	−13.37 dB	−20.34 dB	−14.12 dB	−13.96 dB	−14.38 dB	−13.51 dB	−14.43 dB
Proposed	−19.20 dB	−20.83 dB	−21.17 dB	−20.99 dB	−20.85 dB	−22.85 dB	−22.05 dB	−22.95 dB	−22.70 dB	−22.24 dB	−22.50 dB

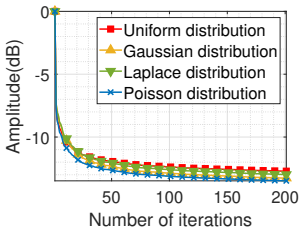

Fig. 1. Convergence speeds.

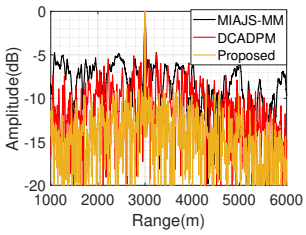

Fig. 2. Range profile.

(17) *by substituting the corresponding input parameters. Specifically, the other three individual operators* $\mathcal{T}\{\mathbf{y}^{(k-1)}, \mathbf{V}_l, \Omega\}$, $\mathcal{T}\{\mathbf{y}^{(k-1)}, \mathbf{V}_0, \{0\}\}$, *and* $\mathcal{T}\{\mathbf{y}^{(k-1)}, \tilde{\mathbf{J}}_0, \{0\}\}$ *can be obtained by replacing* $\{\mathbf{y}^{(k-1)}, \tilde{\mathbf{J}}_l, \Omega_s\}$ *with* $\{\mathbf{y}^{(k-1)}, \mathbf{V}_l, \Omega\}$, $\{\mathbf{y}^{(k-1)}, \mathbf{V}_0, \{0\}\}$, *and* $\{\mathbf{y}^{(k-1)}, \tilde{\mathbf{J}}_0, \{0\}\}$, *respectively.*

Proof. For brevity, let us denote (11a) as $\hat{\zeta}(\mathbf{y})$. Using (9), we can expand $\hat{\zeta}(\mathbf{y})$ in the form as follows

$$\hat{\zeta}(\mathbf{y}) = \epsilon\,\tilde{\delta} \sum_{l\in\Omega_s} |\mathbf{y}^{\mathrm{H}}\tilde{\mathbf{J}}_l\mathbf{y}|^2 + (1-\epsilon)\,\tilde{\delta} \sum_{l\in\Omega} |\mathbf{y}^{\mathrm{H}}\mathbf{V}_l\mathbf{y}|^2 + (1-\delta)\,|\mathbf{y}^{\mathrm{H}}\mathbf{V}_0\mathbf{y}|^2 + \lambda_0\,|\mathbf{y}^{\mathrm{H}}\tilde{\mathbf{J}}_0\mathbf{y} - N|^2. \tag{18}$$

Using Lemma 1, the first term of (18) can be majorized by

$$g_1(\mathbf{y}) = 2\epsilon\tilde{\delta}\Re\Big\{\mathbf{y}^{\mathrm{H}}\Big(\sum_{l\in\Omega_s}\Big(\big((\mathbf{y}^{(k-1)})^{\mathrm{H}}\tilde{\mathbf{J}}_l\mathbf{y}^{(k-1)}\big)^{*}\tilde{\mathbf{J}}_l + (\mathbf{y}^{(k-1)})^{\mathrm{H}}\tilde{\mathbf{J}}_l\mathbf{y}^{(k-1)}\tilde{\mathbf{J}}_l^{\mathrm{H}}\Big) - 2N\mathbf{y}^{(k-1)}(\mathbf{y}^{(k-1)})^{\mathrm{H}} - \sum_{l\in\Omega_s} 2|(\mathbf{y}^{(k-1)})^{\mathrm{H}}\tilde{\mathbf{J}}_l\mathbf{y}^{(k)}|\Big)\mathbf{y}^{(k-1)}\Big\} \tag{19}$$

which is reformulated as $2\epsilon\tilde{\delta}\Re\{\mathbf{y}^{\mathrm{H}}\mathcal{T}\{\mathbf{y}^{(k-1)}, \tilde{\mathbf{J}}_l, \Omega_s\}\mathbf{y}^{(k-1)}\}$ by utilizing the operator $\mathcal{T}\{\cdot,\cdot,\cdot\}$ defined in (17). Similarly, by replacing the set $\{\mathbf{y}^{(k-1)}, \tilde{\mathbf{J}}_l, \Omega_s\}$ of the operator with $\{\mathbf{y}^{(k-1)}, \mathbf{V}_l, \Omega\}$, $\{\mathbf{y}^{(k-1)}, \mathbf{V}_0, \{0\}\}$, and $\{\mathbf{y}^{(k-1)}, \tilde{\mathbf{J}}_0, \{0\}\}$, respectively, the other three components of (18) can be majorized by $g_2(\mathbf{y}) = 2(1-\epsilon)\tilde{\delta}\,\Re\{\mathbf{y}^{\mathrm{H}}\mathcal{T}\{\mathbf{y}^{(k-1)}, \mathbf{V}_l, \Omega\}\mathbf{y}^{(k-1)}\}$, $g_3(\mathbf{y}) = 2(1-\delta)\Re\{\mathbf{y}^{\mathrm{H}}\mathcal{T}\{\mathbf{y}^{(k-1)}, \mathbf{V}_0, \{0\}\}\mathbf{y}^{(k-1)}\}$, and also $g_4(\mathbf{y}) = 2\lambda_0\Re\{\mathbf{y}^{\mathrm{H}}\mathcal{T}\{\mathbf{y}^{(k-1)}, \tilde{\mathbf{J}}_0, \{0\}\}\mathbf{y}^{(k-1)}\}$. Based on the derivation above, we can finally obtain the overall majorant for $\hat{\zeta}(\mathbf{y})$ as presented in (15). The proof is complete. □

Till now, using Lemmas 1 and 2, we can rewrite the k-th sub-problem (11) in the form as

$$\min_{\mathbf{y}} \quad 2\Re\{\mathbf{y}^{\mathrm{H}}\mathbf{Q}^{(k)}\mathbf{y}^{(k-1)}\} \tag{20a}$$

$$\text{s.t.} \quad \|\mathbf{y}\odot\mathbf{u}\|^2 = \gamma_0 N \tag{20b}$$

$$|\mathbf{y}\odot\tilde{\mathbf{u}}| = 1. \tag{20c}$$

The majorization-based update for minimizing the objective (20a) at the k-th iteration can be expressed as

$$\mathbf{s}^{(k)} = -\mathbf{Q}^{(k)}\mathbf{y}^{(k-1)}. \tag{21}$$

For simplicity, let us denote the majorant (15) as $g^{(k)}$. In order to handle the expectation-based objective of (10), we consider minimizing the approximate majorant, which is the weighted average of previously computed majorants. Based on this, the approximate majorant at the k-th iteration is defined as

$$\tilde{g}^{(k)} \triangleq (1-\beta_k)\,\tilde{g}^{(k-1)} + \beta_k\, g^{(k)} \tag{22}$$

where β_k is the weight at the k-th iteration, and its empirical value $\beta_k \triangleq \sqrt{K+1}/\sqrt{K+k}$ has been shown to be effective [12]. Subsequently, by minimizing the approximate majorant (22), the update at the k-th iteration can be given by

$$\bar{\mathbf{s}}^{(k)} = (1-\beta_k)\,\bar{\mathbf{s}}^{(k-1)} + \beta_k\,\mathbf{s}^{(k)}. \tag{23}$$

In order to further improve the convergence rate of our proposed method, we apply an averaging scheme [12] to handle the reformulated convex objective (22). To this end, by defining $\theta^{(k)} \triangleq \sum_{i=1}^{k}\beta_i$, the averaged update can be expressed as

$$\bar{\mathbf{s}}^{(k)} = \big((1-\beta_k)\,\bar{\mathbf{s}}^{(k-1)} + \beta_k\,\tilde{\mathbf{s}}^{(k)}\big)/\theta^{(k)}. \tag{24}$$

After obtaining the averaged update (24), the following task is to conduct proper projections toward (20b) and (20c). For these constraints, we can adjust the magnitudes of vector elements to project to the corresponding feasibility set. Hence, the solution to the k-th sub-problem can be written as

$$\mathbf{y}^{(k)} = \left[\left(\sqrt{\frac{\gamma_0 N}{\|\bar{\mathbf{s}}^{(k)}\odot\mathbf{u}\|^2}}(\bar{\mathbf{s}}^{(k)}\odot\mathbf{u})\right)^{\mathrm{T}}, \left(e^{j\arg(\bar{\mathbf{s}}^{(k)}\odot\tilde{\mathbf{u}})}\right)^{\mathrm{T}}\right]^{\mathrm{T}}. \tag{25}$$

The update procedures (21)–(25) stop when the iteration number k approaches K, which leads to the final solution to (8) given as $\mathbf{y}^{(K)}$. Finally, the detailed algorithm for tackling (8) is summarized in Algorithm 1, with its convergence rate accelerated by the squared iterative method (SQUAREM) [14].

IV. Simulation Results

We evaluate the performance of the proposed algorithm, including its convergence speed under different distributions of ISRJ forwarding times, correlation properties in the single jamming scenario, range profile in the multi-jamming scenario, and the robustness to variations in ISRJ forwarding times. Additionally, we compare our method with the anti-ISRJ algorithms in [7] (namely 'JDA-ADMM'), [8] (namely 'DCADPM'), and [10] (namely 'MIAJS-MM'). Throughout all simulations, we generate sequences with random phases as initialization, and the same initialization is used for fair comparison.

Example 1: Evaluation on convergence speed. We evaluate the convergence speed of the proposed algorithm in terms of normalized objective values versus the number of iterations. To investigate the impact of different probability density functions (PDFs) on the convergence speed, we test several distributions for sampling ISRJ forwarding times within a specified range, including Uniform, Gaussian, Laplace, and Poisson distributions. Other parameters are: $N = 64$, $K = 200$, $\epsilon = 0.5$, $\delta = 0.5$, $\lambda = N$, and $\gamma_0 = 10^{0.2}$. It can be seen from Fig.1 that the proposed algorithm converges to approximately the same value after several iterations for all tested distributions. The results indicate that the proposed algorithm is robust to arbitrary distributions of ISRJ forwarding times.

Example 2: Evaluation on correlation properties. We compare the normalized values of ISL, JIL, JPL, and SINR for all tested algorithms, where the JPL metric represents the peak level of the jamming correlation function [10]. Code lengths selected from the set $\{32, 64, 128\}$ are evaluated, with the preset ISRJ forwarding times set to $m = 20$. The other parameters are the same as used in the previous example. It can be seen from Table I that our proposed algorithm achieves the lowest ISL, JIL, and JPL values, and the highest SINR value across all code lengths. These results demonstrate that the proposed algorithm outperforms all other algorithms in terms of correlation properties and target detection performance.

Example 3: Evaluation on ISRJ suppression. We compare the normalized range profile in the multi-jamming scenario for all tested algorithms. The ISRJ forwarding times are chosen as $m \in \{10, 15, 20\}$, and the location of the real target is set to 3000 m. Other parameters are: $N = 128$, $\epsilon = 0.1$, JSR $= 15$ dB, SNR $= 0$ dB. It can be seen from Fig.2 that the target cannot be identified using MIAJS-MM, while the jamming peak of the range profile obtained by our algorithm is about 5 dB and 8 dB lower than both the jamming peak of DCADPM and the amplitude of the real target, respectively. The results indicate that our method can achieve better anti-ISRJ performance in the multi-jamming scenario, facilitating accurate extraction of real targets at the range bins of interest.

Example 4: Evaluation on parameter sensitivity. We evaluate the parameter sensitivity of all algorithms to ISRJ forwarding times. The preset forwarding times for JDA-ADMM and MIAJS-MM are set to $m = 35$, and the actual ISRJ forwarding times chosen from the set $\{10, 15, 20, 25, 30, 35, 40, 45, 50, 55, 60\}$ are tested. It can be seen from Table II that the JIL values obtained by JDA-ADMM and MIAJS-MM vary with ISRJ forwarding times, with the maximum and minimum values differing by approximately 12 dB and 10 dB, respectively. In contrast, the JIL values obtained by our algorithm fluctuate within a range of no more than 3 dB. The results indicate that when there is a deviation in forwarding times, the anti-ISRJ performance of MIAJS-MM and JDA-ADMM significantly decreases, while our algorithm can maintain the robustness to varying ISRJ forwarding times.

V. Conclusion

We have proposed an algorithm for jointly designing the unimodular waveform and the mismatched filter with excellent ISRJ suppression capability and robustness to forwarding times. Specifically, we have formulated a non-convex problem with constraints on SNRL and mainlobe peak level, and have reformulated its objective into an expected form with respect to forwarding times. To solve it, we have decomposed the expectation-based problem into a set of sub-problems. Then, we have reformulated each sub-problem into a quadratic form, chosen a proper majorant for each distinct objective, and finally derived a closed-form solution via the SMM technique. Simulation results verify the effectiveness of our design.

References

[1] D. Feng, L. Xu, X. Pan, and X. Wang, "Jamming wideband radar using interrupted-sampling repeater," *IEEE Trans. Aerosp. Electron. Syst.*, vol. 53, no. 3, pp. 1341–1354, 2017.

[2] L. Neng-Jing and Z. Yi-Ting, "A survey of radar ecm and eccm," *IEEE Trans. Aerosp. Electron. Syst.*, vol. 31, no. 3, pp. 1110–1120, 1995.

[3] X. Wang, J. Liu, W. Zhang, Q. Fu, Z. Liu, and X. Xie, "Mathematic principles of interrupted-sampling repeater jamming (isrj)," *Sci. China, Ser. F: Info. Sci.*, vol. 50, pp. 113–123, 2007.

[4] C. Zhou, Q. Liu, and X. Chen, "Parameter estimation and suppression for drfm-based interrupted sampling repeater jammer," *IET Radar, Sonar & Navigation*, vol. 12, no. 1, pp. 56–63, 2018.

[5] T. Guo, H. Zhan, X. Su, and T. Wang, "Anti-interrupted sampling repeater jamming method for random pulse repetition interval and intra-pulse frequency agile radar," *IET Radar, Sonar & Navigation*, vol. 17, no. 12, pp. 1796–1811, 2023.

[6] R. Zhang, Y. Shen, S. Qiu, J. Yu, and W. Sheng, "Polyphase waveform design for isrj suppression based on l-bfgs method," *Digit. Signal Process.*, vol. 133, p. 103840, 2023.

[7] K. Zhou, D. Li, Y. Su, and T. Liu, "Joint design of transmit waveform and mismatch filter in the presence of interrupted sampling repeater jamming," *IEEE Signal Process Lett.*, vol. 27, pp. 1610–1614, 2020.

[8] M. Ge, X. Yu, Z. Yan, G. Cui, and L. Kong, "Joint cognitive optimization of transmit waveform and receive filter against deceptive interference," *Signal Process.*, vol. 185, p. 108084, 2021.

[9] K. Zhou, D. Li, S. Quan, T. Liu, Y. Su, and F. He, "Sar waveform and mismatched filter design for countering interrupted-sampling repeater jamming," *IEEE Trans. Geosci. Remote Sens.*, vol. 60, pp. 1–14, 2021.

[10] Y. Gao, H. Fan, L. Ren, Z. Liu, Q. Liu, and E. Mao, "Joint design of waveform and mismatched filter for interrupted sampling repeater jamming suppression," *IEEE Trans. Aerosp. Electron. Syst.*, 2023.

[11] H. Su, Q. Bao, J. Pan, F. Guo, and W. Hu, "Waveform domain adaptive matched filtering for suppressing interrupted sampling repeater jamming," *IEEE Trans. Aerosp. Electron. Syst.*, 2024.

[12] J. Mairal, "Stochastic majorization-minimization algorithms for large-scale optimization," *Adv. Neur. In.*, vol. 26, 2013.

[13] J. Song, P. Babu, and D. P. Palomar, "Sequence design to minimize the weighted integrated and peak sidelobe levels," *IEEE Trans. Signal Process.*, vol. 64, no. 8, pp. 2051–2064, 2015.

[14] R. Varadhan and C. Roland, "Simple and globally convergent methods for accelerating the convergence of any em algorithm," *Scand. J. Stat.*, vol. 35, no. 2, pp. 335–353, 2008.